

Enhancing the harvesting of sunlight by exploiting its spatial coherence

Pedro Manrique¹, Adriana De Mendoza², Felipe Caycedo-Soler³, Ferney Rodríguez², Luis Quiroga²
and Neil Johnson¹

¹*Physics Department, University of Miami, Coral Gables, Florida FL 33126, U.S.A.*

²*Departamento de Física, Universidad de Los Andes, A.A. 4976, Bogotá, Colombia*

³*Institute of Theoretical Physics, University of Ulm,
Albert-Einstein-Allee 11, D - 89069 Ulm, Germany*

(Dated: March 22, 2022)

A key goal of energy science is to enhance the harvesting of sunlight in artificial and natural systems. Spatial coherences in the incident sunlight are typically assumed to be of negligible benefit, and are ignored in current designs. Here we show, however, that such spatial correlations can be exploited to enhance the trapping of sunlight, as well as providing a potential driving mechanism for self-organized photosynthetic systems. Our theory is grounded by empirical inputs, while its output is validated against testable predictions.

There have been many efforts to enhance the capture of energy from sunlight through novel photosynthetic designs and materials. Much of this focus is concentrated on capturing the amplitude of the light field, without paying attention to the spatial correlations that are embedded within it. Indeed, the nature and possible uses of the quantum-mechanical correlations within light continue to generate heated debates. While the photoelectric effect establishes that light transfers energy to materials through the capture of individual energy packets (photons), experiments probing Bell inequalities and Hanbury-Brown-Twiss effects show that photons can also exhibit highly non-trivial spatial correlations – even within natural sunlight[1]. A fundamental open question concerns the extent to which such correlations might be exploited[2, 3]. The study of coherent effects in light-driven biological systems has attracted increasing attention due to the observation of long-lasting oscillatory signals measured with time-resolved techniques [4–6]. Although there has been a subsequent wave of theoretical works concentrated on these systems’ excitonic and vibrational properties[7, 8], they have all overlooked the effect of the correlations present in the incident light. Yet the nontrivial correlations within thermal light, which is light from a source at a particular temperature, is already known to generate a variety of unexpected effects, including sub-wavelength interference[9], ghost imaging[10] and photon-number correlations[11]. The transverse coherence length for natural sunlight has been both estimated for a quasi-monochromatic beam (for a wavelength of $\bar{\lambda} \sim 500\text{nm}$)[12] and measured for broadband solar beam radiation[13] as $60\mu\text{m}$ and $200\mu\text{m}$, respectively. Therefore photosynthetic systems within this length-scale range – whether natural or artificial – should experience the spatial coherence present within sunlight and other light sources.

Our findings show quantitatively that spatial correlations in incident light – specifically thermal light – can be used to enhance the efficiency and robustness of light harvesting. We show that the organization of harvest-

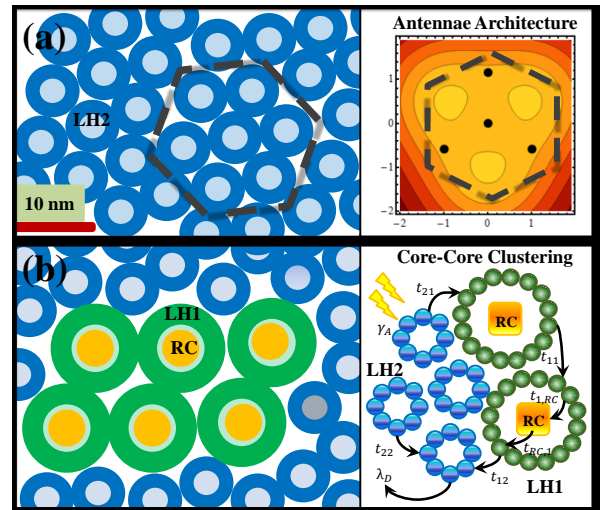


FIG. 1: Typical antennae organization of low-light adapted photosynthetic purple bacteria. (a) Schematic representation of real AFM images of low-light adapted native membrane of *Rsp. photometricum* displaying LH2 hexagonal packing[28] and probability of detecting 4 photons by a configuration of five antennae. The latter shows an optimal arrangement for hexagonal architecture. (b) Schematic representation of real AFM images of *Rhodobacter sphaeroides*[19] showing high core-core clustering, and our theoretical model of excitation transfer and RC ionization.

ing units complements the spatial correlations naturally present in sunlight. Specifically we find that hexagonal crystalline arrays of harvesting units optimize photon absorption (Fig. 1(a)), a fact that hints at an efficient yet photo-protective role for the different macro-molecular assemblies in natural systems. Furthermore we show that the macro-molecular aggregation of harvesting structures displays a high sensitivity to these spatial correlations in the incident light, which in turn benefits the charge separation process in architectures that happen to be compatible with those observed in natural structures (Fig. 1(b)).

Our goal here is a proof-of-principle that can be ap-

plied to future energy-harvesting photosynthetic designs, whether these be engineered or self-organized – perhaps even biological. We therefore consider the simplest possible setup for a primitive photosynthetic system: sunlight (i.e. thermal light from a blackbody emitter) incident on N pigments (individual or aggregates) that can each absorb a photon and transfer the energy to a neighboring unit. Such pigments are present in all photosynthetic systems[14–19]. We focus our modeling on monochromatic polarized thermal light, though our findings generalize to multiple frequencies and polarizations. We start by considering photo-excitations arising in a time interval (τ) that is shorter than the coherence time of the light (τ_c) – however we have checked (see Supplementary Material SM) that the main findings are robust to detection times that are a factor of 100 or higher than τ_c (for a wavelength range between 855 and 895nm, $\tau_c = 400$ fs [12]). The joint probability $P(n_1, n_2, \dots, n_N)$ that n_i photo-excitations will be registered by the i 'th antenna ($i = 1, \dots, N$) is related to the generating function $G(s_1, s_2, \dots, s_N) = G(\{s_i\})$ [20] (see SM). The second-order degree of coherence of the radiation field between antennae located at \vec{r}_i and \vec{r}_j is denoted as $g_{i,j}$ and $\langle n_i \rangle$ is the average number of photo-counts at the i 'th antenna. The latter is directly connected with the mean intensity ($\langle I_i \rangle$) through the relation $\langle n_i \rangle = \alpha_i \langle I_i \rangle \tau$, where α_i is the quantum efficiency of the i 'th antenna. Notice that both domain sizes in organic solar cells [21] and those of natural photo-receptive harvesting vesicles like those from purple bacteria[14, 22–24] which are among the first examples of photosynthetic membranes formed on Earth, present a typical length of $\simeq 200$ nm, hence will be entirely contained inside the coherence area of sunlight[13].

The probability of detection of $n = \sum_i n_i$ photons regardless of the specific counting record of any individual antenna, is (see SM):

$$P(n) = \frac{(-1)^n}{n!} \frac{\partial^n}{\partial s^n} \{ \text{Det} [\hat{1} + \langle n \rangle s \hat{g}] \}_{s=1}^{-1} \quad (1)$$

where $\hat{1}$ and \hat{g} are the $N \times N$ identity and second-order degree of coherence matrices respectively. For thermal radiation, the latter is registered by detectors placed at \vec{r}_i and \vec{r}_j , i.e. $g_{i,j}$, obeys the analytical expression[12, 25]

$$g_{i,j} = \frac{2J_1(u_{i,j})}{u_{i,j}} \quad (2)$$

where $J_1(z)$ is a Bessel function, $u_{i,j} = \kappa |\vec{r}_i - \vec{r}_j|$ is the effective ratio between the detectors' separation and the spatial coherence length, with κ depending on the average wavelength, the size of the source and source-detector separation. Two limiting cases illustrate the important impact of spatially correlated photons: (1) Full spatial coherence, where the area contained by the N antennae is much smaller than the coherence area of the thermal light ($g_{i,j} = 1$ for any pair of detectors). This yields the Bose-Einstein distribution in the number of excitations (see

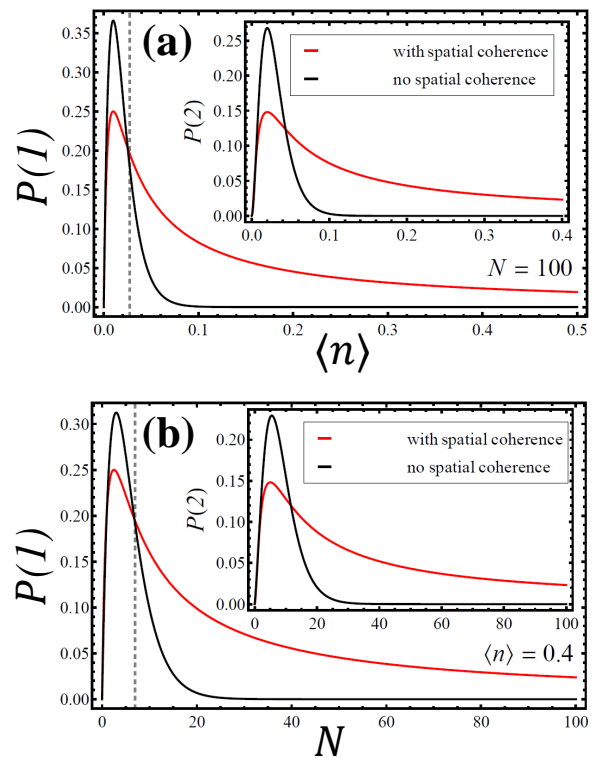


FIG. 2: Effects of spatial coherence on photo-detection statistics. Probability of detection of one photon $P(1)$ as a function of (a) intensity $\langle n \rangle$ for a cluster of $N = 100$ antennae, and (b) number of antennae (N) for a fixed intensity ($\langle n \rangle = 0.4$). Red lines correspond to full spatial coherence, i.e. $g_{i,j} = 1$. Black lines correspond to no spatial coherence, i.e. $g_{i,j} = 0$ with $i \neq j$. Dashed lines indicate the crossing points between the full coherence and incoherence description at (a) $\langle n \rangle = 0.025$ and (b) $N = 7$. Insets show the probability for detecting photon pairs, $P(2)$.

SM) where the average excitation number $\tilde{n} = N \langle n \rangle$, and with the exciting light able to display non-classical correlations, e.g. the Hanbury-Brown-Twiss effect[12, 26, 27]. (2) No spatial coherence, i.e. $g_{i,j} = 0$ where $i \neq j$ with the distance between any two antennae being larger than the spatial coherence length of the thermal light. The resulting two-parameter distribution only reduces to the Poisson distribution in the limits $N \rightarrow \infty$ and $\langle n \rangle \rightarrow 0$ with $\tilde{n} = N \langle n \rangle = \text{constant}$.

Figure 2 shows explicitly how the incident light's spatial correlations impact the probability of photon detection by the N antennae. Different light intensities are particular to the specific niche of the photosynthetic organism. For a wide range of $\langle n \rangle$ (i.e., $\langle n \rangle \geq 0.025$ in Fig. 2(a)) and for antennae that are clustered within the coherence radiation area as in realistic photosynthetic membranes ($N > 7$ in Fig. 2(b)), the probabilities for 1 and 2-photon detection are consistently higher for spatially coherent light than for fully incoherent light (see Fig.S1 for multiple photons). These probabilities are

fairly insensitive to fluctuations in $\langle n \rangle$ and N and hence offer robustness protection to the underlying membrane, against atmospheric variations and the recurrent photo-bleaching of pigments. The fact that the probability distribution with full spatial coherence is greater than that for no spatial coherence across essentially the full range of \tilde{n} , proves that the coherence of sunlight will increase the photo-detection.

We now analyze the effect of spatial coherence on simple antennae architecture motifs from which larger membrane or organic cell structures, both natural or artificial, can in principle be built. Figure 3 illustrates the photo-count statistics for a configuration of five antennae and three values of light intensity. The configuration consists of three antennae in an equilateral triangle and a fourth one at the center. The probabilities of detecting $n = 1, 2$ and 3 photons are calculated as a function of the position of the fifth antenna. The configuration of photo-detectors (Fig. 3) that maximizes the underlying probability associated with a specific number of photo-detections, is remarkably similar to the honeycomb architecture found in several species of purple bacteria[22, 24, 28, 29]. The number of photons n , whose probability is maximized, is directly related to the light intensity. Importantly, for light intensity characterized by $\langle n \rangle = 0.5$, the honeycomb architecture maximizes the probability of detecting one photon (Fig. 3(a)). Interestingly, for larger light intensities, the honeycomb architecture maximizes the probability of detecting a larger number of photons. For example, for $\langle n \rangle = 1$ and $\langle n \rangle = 1.45$, the detection of two (Fig. 3(b)) and three (Fig. 3(c)) photons by a hexagonal architecture is optimal, respectively. This suggests that the honeycomb para-crystalline domains of antennae complexes observed in membranes under low light intensity, where $\langle n \rangle < 0.5$, may benefit from single photon absorption. In addition, photo-protection in high light intensity environments by means of a reduced absorption of single photons, might be achieved by amorphous macro-molecular assemblies. These statements are consistent with the observed chromatic adaptation of the antennae complexes to the light intensity during the growing stage[14, 24, 30], where a transition from para-crystalline domains to amorphous structures of harvesting complexes is also reported. However, our findings suggest that the photosynthetic apparatus adapts to both the incident light's intensity and correlations. By contrast, in the case of no spatial coherence, there is no preferred position for the fifth detector and hence the light offers no guiding organizational principle (see SM).

Having established the impact of light's spatial coherence on photon absorption for highly primitive geometric motifs, we now examine the effects for actual architectures in purple bacteria (e.g. Fig.1(b) corresponding to *Rb. sphaeroides*[19]). The membrane's performance is quantified by its efficiency η , defined as the ratio of photo-excitations that produce charge separation in the

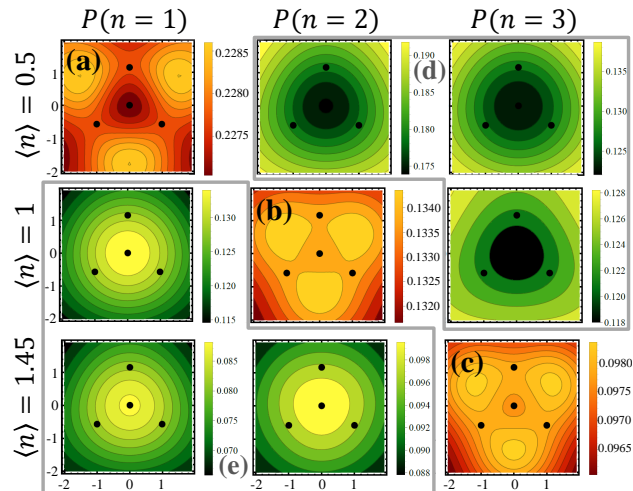


FIG. 3: Numerical evaluation of the full joint probability for $N = 5$ antennae. The value of $P(n)$ is plotted as a function of the position of the 5'th detector in the $x - y$ plane, with the remaining 4 antennae fixed in space (large black dots). Diagonal plots show the hexagonal arrangement optimization for detecting (a) one, (b) two and (c) three photons. Off diagonal plots show preference for the fifth detector to be in (d) the periphery and (e) the center of the configuration. The dimensionless distance between nearest neighbor detectors is fixed to $u = 1$ (see Eq. (2)) and all distances in the $x-y$ plane are measured in terms of this inter-detector distance.

RCs, to the total number of absorbed photons. Similarly we define the relative efficiency η/η_{RA} , to compare the efficiency η of correlated photons and the efficiency η_{RA} for the scenario where spatial correlations are not accounted for. We study membranes which have the same number of LH1 and LH2 complexes, but differ in the specific architecture/configuration of complexes; in particular, the RC-LH1 core-core clustering. Hence the contrasting situations of high core-core clustering (HCC, Fig.4(a)) and sparse low core-core clustering (LCC, Fig.4(b)), differ in terms of the mean number of RC-LH1 which encircle any RC-LH1 core-complex. Figure 4(a) represents well the maximal core-core clustering that is observed in *Rsp. photometricum* for low-light intensity growth[23] with a linear core arrangement similar to *Rb. sphaeroides*[19], while Fig.4(b) resembles the vesicles grown under high-light intensity in *Rsp. photometricum*[23].

Our semiclassical model places consecutive absorptions within a correlation radius r in order to simulate the spatial bunching of thermal light. The resultant excitation diffuses until either dissipation occurs or an RC is reached and charge separation takes place. The RCs might be available to produce charge separation depending on whether an average time τ_{RC} (of a few milliseconds) has elapsed after the previous charge separation in that specific RC occurred (see SM and Ref. 18). The RC cycling successfully explains structural preferences in adaptation of purple bacteria[14, 24, 30]. Figure 4(c)

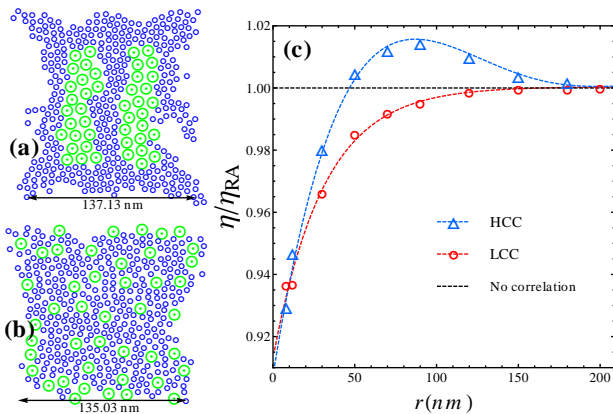


FIG. 4: Metabolic implications of spatially correlated photon arrival. Architectures of the antenna complexes (a) HCC and (b) LCC. They are obtained as local minima in a large-scale Monte Carlo energy minimization, and are hence realistic as (locally stable) minimum energy structures. Blue rings represent LH2 antennae and green rings are core RC-LH1 complexes. (c) Photosynthetic relative efficiency as a function of the correlation parameter r for architectures HCC (triangles) and LCC (circles). Dashed black line illustrates the result without light correlation. Symbols represent the result from our model while lines correspond to the fitting of our simulation points. The RC closure time is $\tau_{RC} = 12.5$ ms.

shows the striking result that HCC membranes benefit from the spatial correlations present in the incident sunlight. Our model captures a peak enhancement in the photosynthetic efficiency for membranes with HCC clustering (blue triangles), which is however absent in the LCC (red circles). Our simulations reveal that HCC presents a reduction in the number of complexes visited before charge separation takes place, when consecutive absorptions occur within radii compatible with the core clusters size. This can be understood as a benefit of placing clustered cores in the presence of the incident thermal light which is spatially bunched. Therefore it is desirable to envision clustered charge separation units for efficient conversion in artificial devices subject to sunlight excitation.

While other energetic and metabolic factors (e.g. complexes affinity and charge carrier diffusion) may ultimately dictate a given membrane's architecture in a given environment, our results also speak to open questions about the purpose of membrane organization[19, 22], showing that it allows the system to harvest not only the light's energy, but also to profit from its spatial correlations. The increment in efficiency shown in Fig.4(c) should not be regarded as negligible: It has been demonstrated that for these organisms, large structural variations occur as a result of seemingly modest metabolic benefits. For example, *Rsp. acidophila* develops an ex-

pensive structural adaptation under low intensity illumination that gradually replaces LH2 by LH3 complexes which, due to a red shifted maximum, improves the transfer to the LH1 which in turn improves the membrane's efficiency by 3-4%[17]. For negative spatial correlation in the incident light (i.e. opposite of natural light), the peak disappears as shown in Fig. S3 of SI.

In summary, we have explored how the geometry of light-harvesting units and the statistical properties of incident thermal light, influence energy absorption. We have shown that absorption in harvesting units set in honeycomb crystal lattices benefits from thermal sources, and that these assemblies closely resemble the observed natural aggregation of purple bacteria photosynthetic membranes grown under low light intensity conditions. By contrast, such a finding hints at a photo-protection role for any amorphous aggregation of harvesting structures in purple bacteria grown under higher light intensity regimes. Finally, we have shown that clustering of charge separation units might be used to exploit the spatial correlation of thermal light by means of reducing the mean free path required for absorbed excitations to reach a charge separation unit.

-
- [1] Ragy, S. and Adesso, G. Nature of light correlations in ghost imaging. *Scientific Reports* **2** 651; DOI:10.1038/srep00651 (2012).
 - [2] Sim, N. et al., Measurement of Photon Statistics with Live Photoreceptor Cells. *Phys. Rev. Lett.* **109**, 113601 (2012).
 - [3] Brumer, P. et al., Molecular response in one-photon absorption via natural thermal light vs. pulsed laser excitation. *Proceedings of the National Academy of Sciences* **109**, 48:19575-19578 (2012).
 - [4] Engel, G.S. et al., Evidence for wavelike energy transfer through quantum coherence in photosynthetic systems. *Nature* **446**, 782-786 (2007).
 - [5] Collini, E. et al. Coherently wired light-harvesting in photosynthetic marine algae at ambient temperature. *Nature* **463**, 644-647 (2010).
 - [6] Romero, E. et al. Quantum coherence in photosynthesis for efficient solar-energy conversion. *Nature Physics* **10**, 676-682 (2014).
 - [7] Christensson, N., Kauffmann, H. F., Pullerits, T. and Mancal, T. Origin of long-lived coherences in light-harvesting complexes. *J. Phys. Chem. B* **16**, 7449-7454 (2012).
 - [8] Chin, A.W., et al. The role of non-equilibrium vibrational structures in electronic coherence and recoherence in pigment protein complexes. *Nature Physics* **9**, 113-118 (2013).
 - [9] Cao, D. Z., Ge, G. J. and Wang, K. Two-photon sub-wavelength lithography with thermal light. *Appl. Phys. Lett.* **97**, 051105 (2010).
 - [10] Zhou, Y., Simon, J., Liu, J. and Shih, Y. Third-order correlation function and ghost imaging of chaotic thermal light in the photon counting regime. *Phys. Rev. A* **81**,

- 043831 (2010).
- [11] Chen, H., Peng, T. and Shih, Y. 100% correlation of chaotic thermal light. *Phys. Rev. A* **88**, 023808 (2013).
- [12] Mandel, L. and Wolf, E. *Optical coherence and Quantum Optics*. (Cambridge University Press, Cambridge, 1995).
- [13] Mashaal, H., Goldstein, A., Feuermann, D. and Gordon J.M. First direct measurement of the spatial coherence of sunlight. *Optics Letters* **37**, 17 (2012)
- [14] Scheuring, S. and Sturgis, J. N. Chromatic adaptation of photosynthetic membranes. *Science* **309**, 484-487 (2005).
- [15] Blankenship, R. *Molecular Mechanisms of Photosynthesis*. (Wiley-Blackwell, Tempe, 2002).
- [16] Scholes, G., Fleming, G., Olaya-Castro, A. and van Grondelle, R. Lessons from nature about solar light harvesting. *Nature Chemistry* **3**, 763774 (2011)
- [17] Hu, X., Ritz, T., Damjanovic, A., Autenrieth, F. and Schulten, K. Photosynthetic apparatus of purple bacteria. *Quarterly Reviews of Biophysics* **35**, 1-62 (2002)
- [18] Caycedo-Soler, F., Rodriguez, F. J., Quiroga, L. and Johnson, N. F. Light-Harvesting Mechanism of Bacteria Exploits a Critical Interplay between the Dynamics of Transport and Trapping. *Phys. Rev. Lett.* **104**, 158302 (2010).
- [19] Bahatyrova, S., et al. The native architecture of a photosynthetic membrane. *Nature*, **430**, 1058-1062 (2004)
- [20] Zardecki, A. Application of the Functional Formalism to Investigation of the Photoelectric Counting Distribution. *Can. J. Phys.* **49**, 1724-1730 (1971).
- [21] Collins, B. A, Li, Z, Tumbleston, J.R., Gann, E., McNeill C.R., and Ade, H. Absolute measurement of domain composition and nanoscale size distribution explains performance in PTB7:PC71BM solar cells, *Advanced Energy Materials* **3**, 65 (2013).
- [22] Simon Scheuring, S. and Sturgis, J. N. Dynamics and Diffusion in Photosynthetic Membranes from *Rhodospirillum Photometricum*. *Biophys. J.* **91**, 3707-3717 (2006)
- [23] Scheuring, S., Rigaud, J. L. and Sturgis, J. N. Variable LH2 stoichiometry and core clustering in native membranes of *Rhodospirillum photometricum*. *EMBO J.* **23**, 4127-4133 (2004)
- [24] Scheuring, S., Goncalves, R. P., Prima, V. and Sturgis, J. N. The Photosynthetic Apparatus of *Rhodospseudomonas palustris*: Structures and Organization. *Journal of Molecular Biology.* **358**, 83-96 (2006)
- [25] Cantrell, C. D. and Fields, J. R. Effect of Spatial Coherence on the Photoelectric Counting Statistics of Gaussian Light. *Phys. Rev. A* **7**, 2063-2069 (1973).
- [26] Hanbury Brown, R. and Twiss, R. Q. Interferometry of the Intensity Fluctuations in Light. I. Basic Theory: The Correlation between Photons in Coherent Beams of Radiation. *Proc. R. Soc.* **A242**, 300-324 (1957);
- [27] Hanbury Brown, R. and Twiss, R. Q. Interferometry of the Intensity Fluctuations in Light II. An Experimental Test of the Theory for Partially Coherent Light *Proc. R. Soc.* **A243**, 291-319 (1958).
- [28] Sturgis, J. and Niedermann R. Atomic force microscopy reveals multiple patterns of antenna organization in purple bacteria: implications for energy transduction mechanisms and membrane modeling. *Photosynth Res.* **95** 269-278 (2008)
- [29] Karrasch, S., Bullough, P.A. and Ghosh, R. The 8.5Å projection map of the light-harvesting complex 1 from *Rhodospirillum rubrum* reveals a ring composed of 16 subunits. *EMBO J.* **14**, 631-638 (1995).
- [30] Adams, P. G. and Hunter, C. N. Adaptation of intracytoplasmic membranes to altered light intensity in *Rhodobacter sphaeroides*. *Biochimica et Biophysica Acta* **1817**, 1616-1627 (2012)